Supplementary material

Heterojunction-Driven MXenzyme Biocatalysis: A Progressive Strategy to Remodel Tumor Immune Microenvironment for Improved Therapeutic Efficacy

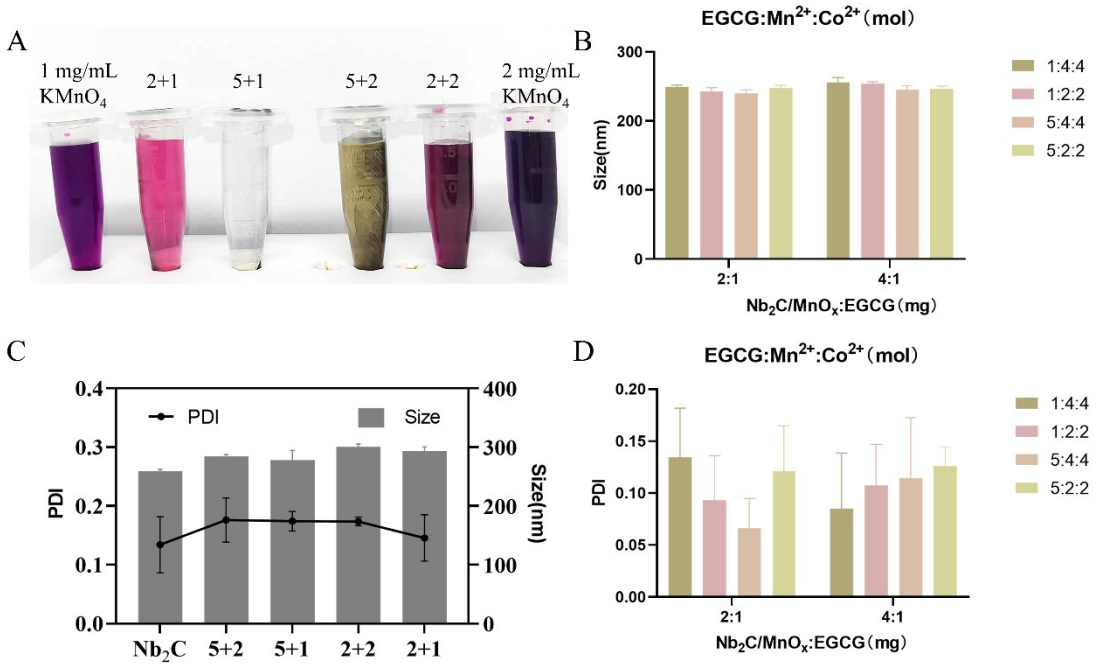

Fig. S1. Synthesis of NbM@EDM. (A) Photographs of the supernatant after centrifugation of NbM under different preparation conditions. (B) Particle size and PDI of NbM under different preparation conditions. (C) Particle size of NbM@EDM under different preparation conditions. (D) PDI of NbM@EDM under different preparation conditions.

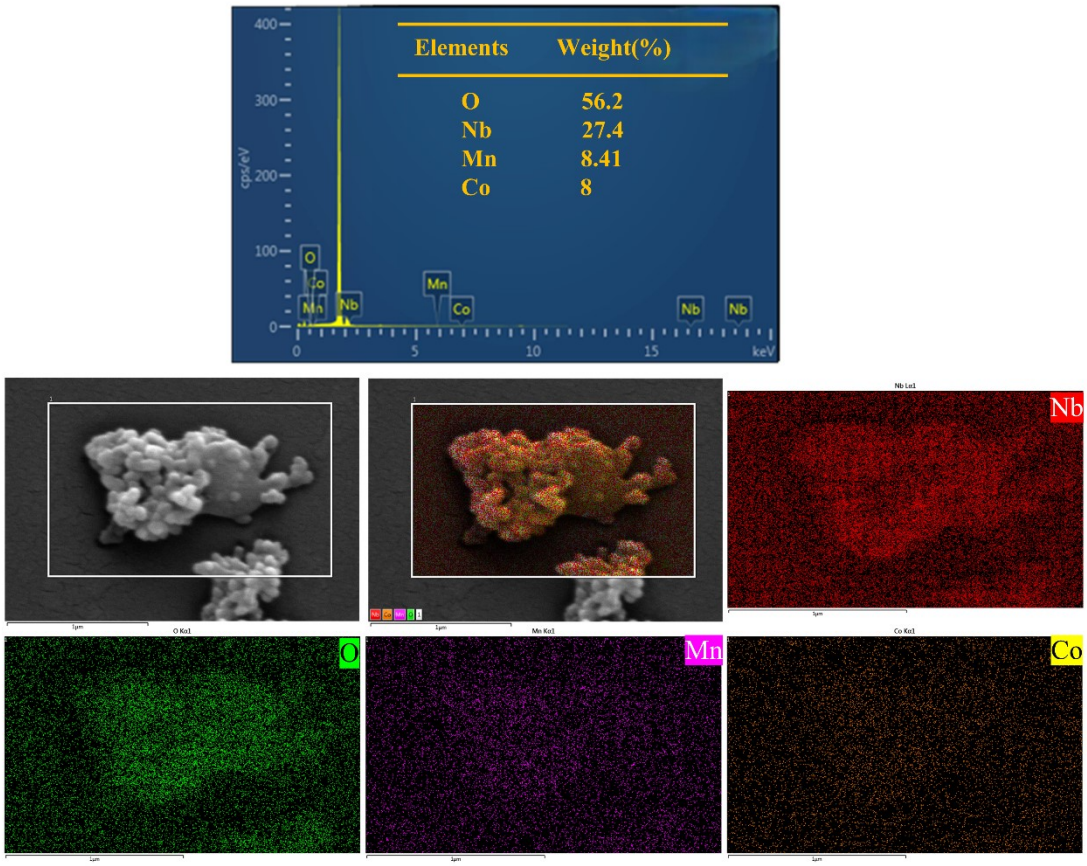

Fig. S2. SEM photographs and element mapping of NbM@EDM.

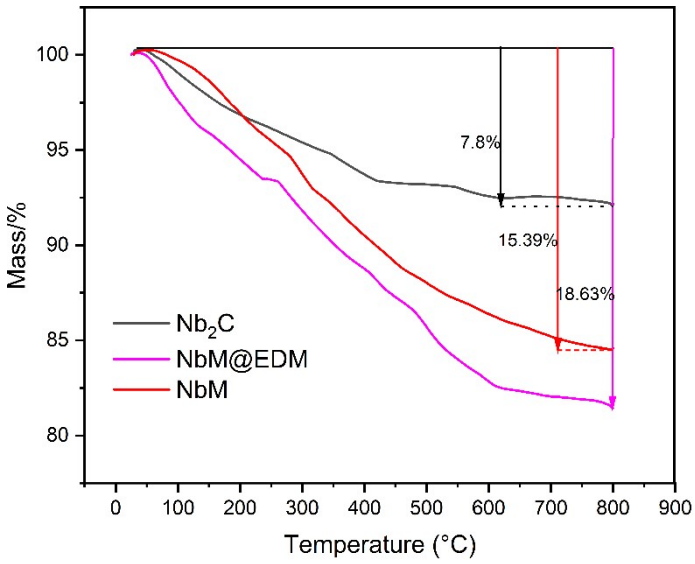

Fig. S3. TGA images of Nb_2C, NbM and NbM@EDM.

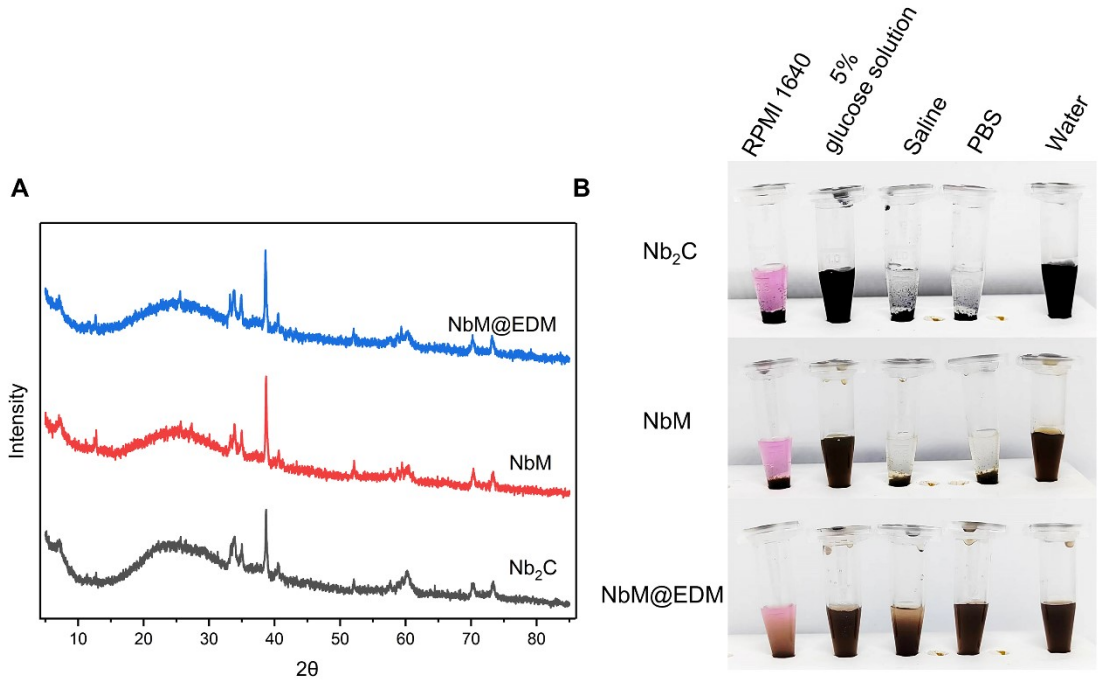

Fig. S4. Characterization of NbM@EDM. (A) XRD images of Nb2C, NbM and NbM@EDM. (B) Stability of NbM@EDM under different media (24h).

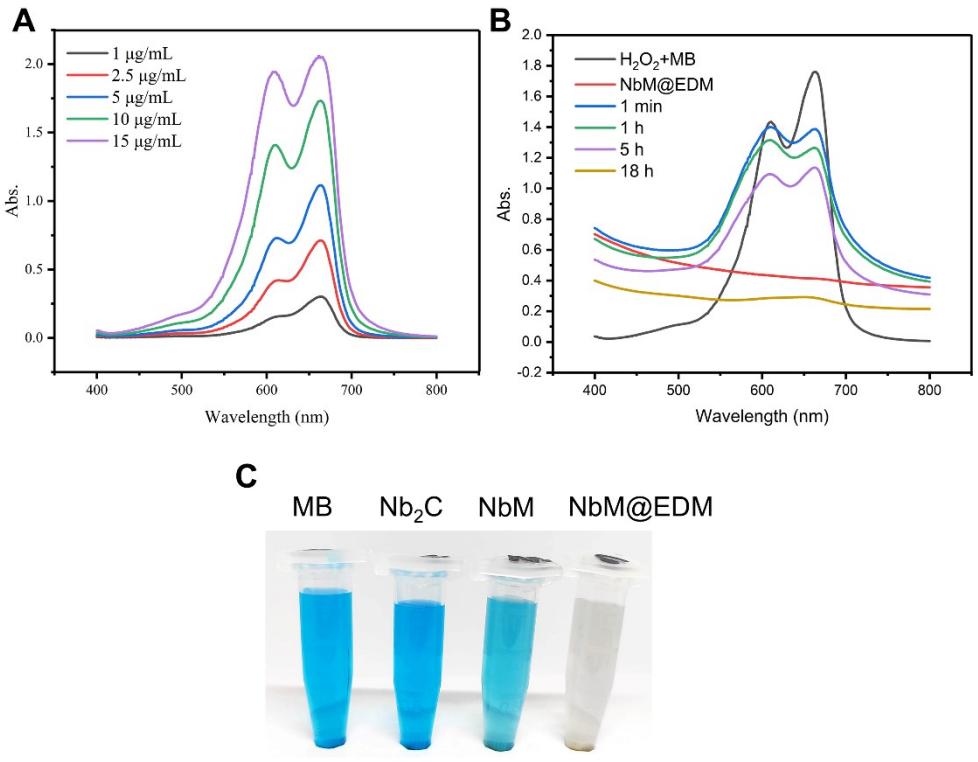

Fig. S5. Absorption curves of NbM and NbM@EDM nanoparticles mixed with MB solution. (A) Absorption curves of MB solutions with different concentrations. (B) Photocurrent responses of Absorption curves of NbM@EDM nanoparticles mixed solution with MB. (C) Photograph of the color of the mixed solution after the nanoparticles were mixed with MB and incubated for some time.

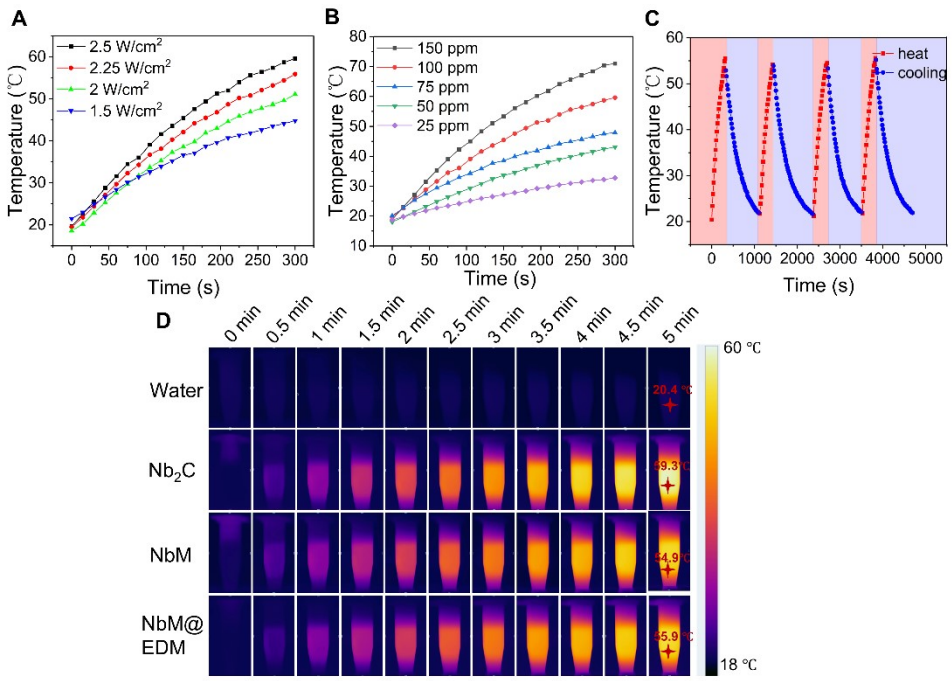

Fig. S6. Evaluation of the photothermal performance. (A) Photothermal warming curves of NbM@EDM at different power densities (1.5 W/cm^2, 2 W/cm^2, 2.25 W/cm^2, 2.5 W/cm^2) and (B) different concentrations (25 ppm, 50 ppm, 75 ppm, 100 ppm and 150 ppm). (C) *In vitro* thermal images of different nanoparticle suspensions (2.25 W/cm^2， 100 ppm) under laser irradiation. (D) Photo-thermal stability of NbM@EDM nanoparticles.

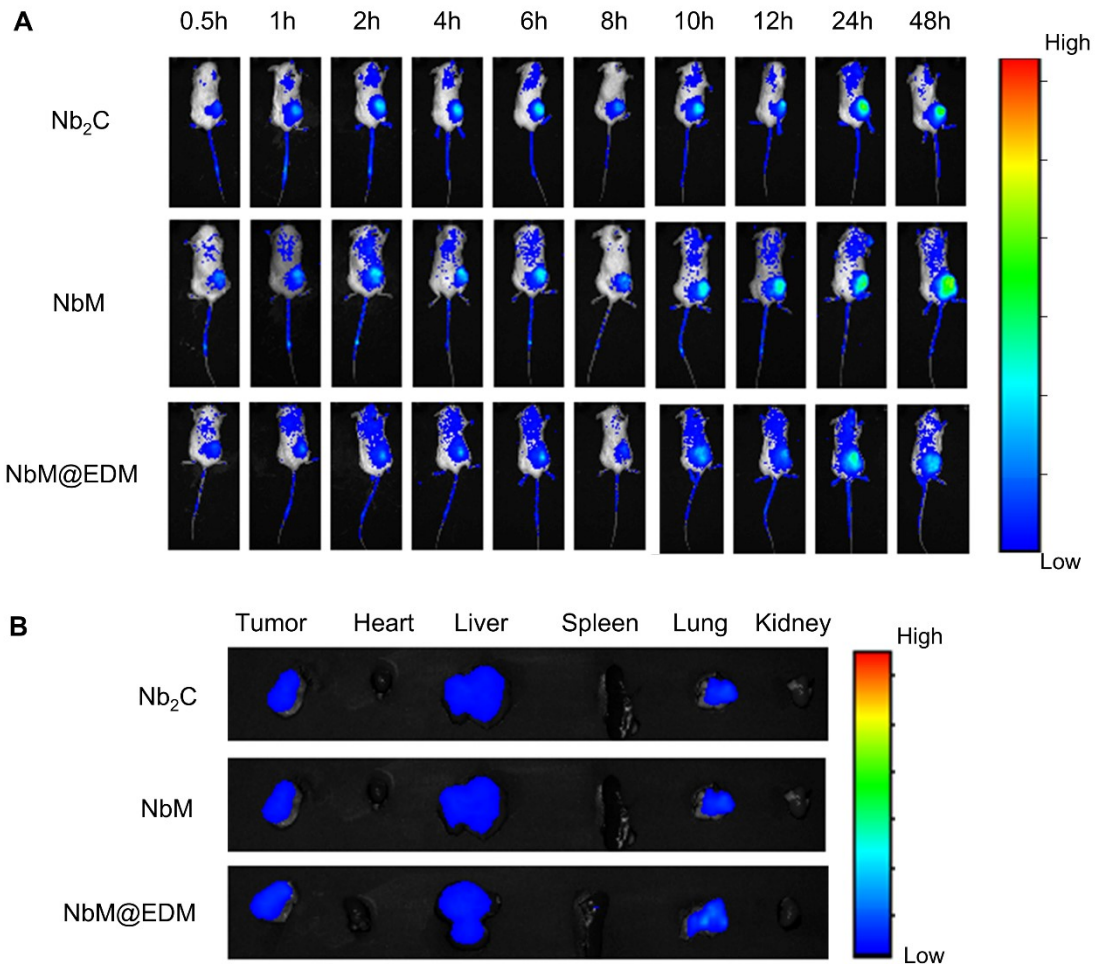

Fig. S7. In vivo distribution of the nanoparticles.

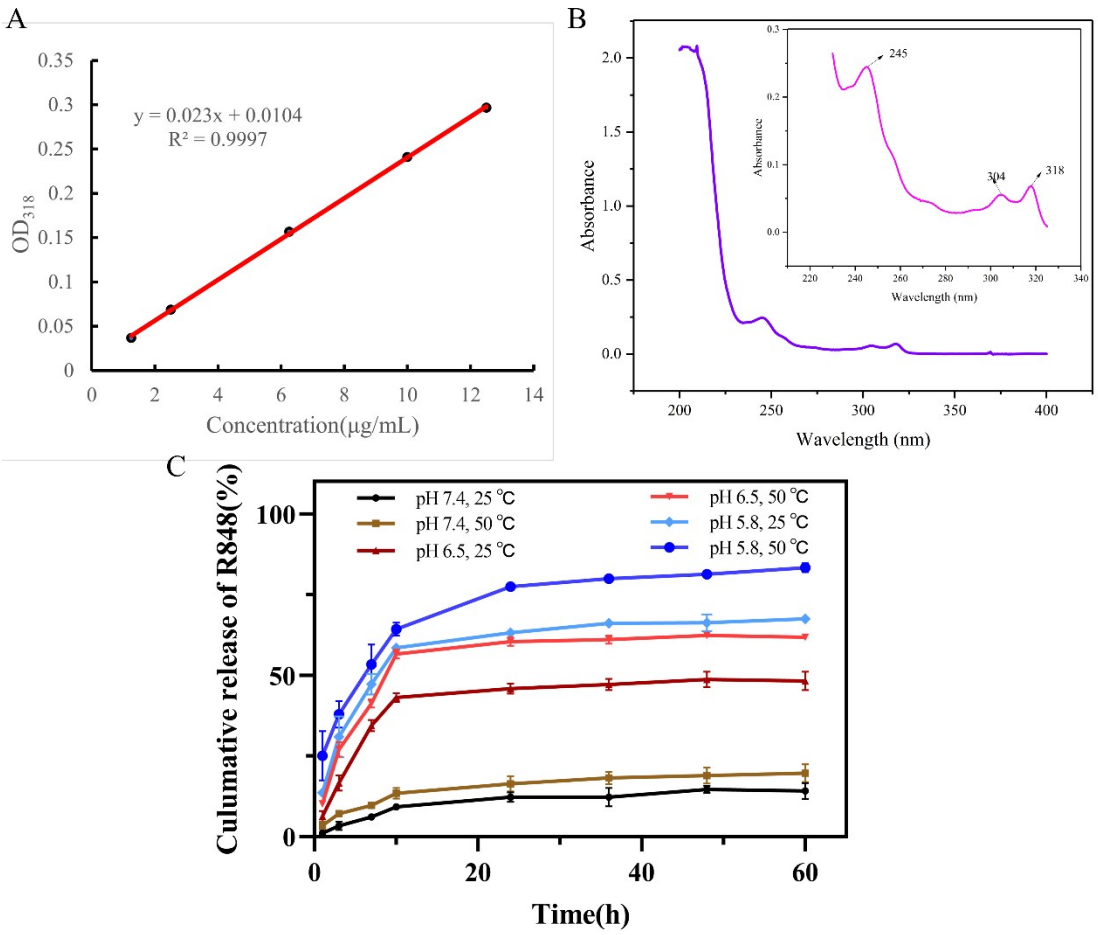

Fig. S8. Calculation of LC rate and EE. (A) Absorption spectrum of R848 in the range of 190-400 nm. (B) Standard curve of R848. (C) In vitro drug release behavior of NbMR@EDM under different media and temperature conditions.

The supernatant collected after the initial centrifugation of NbM@R848 underwent a second centrifugation to ensure complete removal of NbM nanoparticles. This second centrifugation was carried out at the highest possible speed and for the longest duration to minimize the absorption of NbM nanoparticles at 318 nm to nearly zero. Subsequently, we used the standard curve of R848 to calculate the encapsulation

efficiency (EE) and loading capacity (LC) of the nanoparticles as 94.53% and 8.01% respectively.

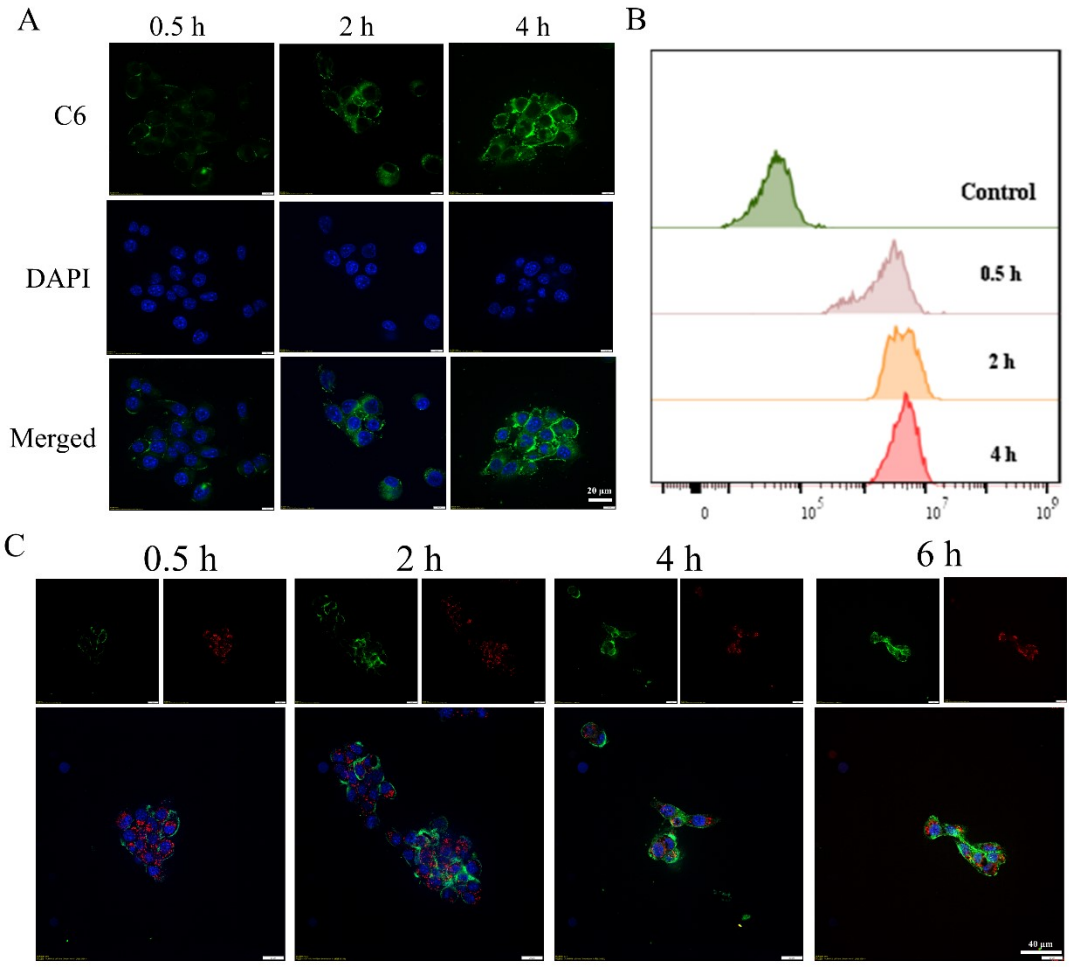

Fig. S9. Uptake behavior of nanoparticles by tumor cells. (A) Confocal microscopy and (B) flow cytometry detection of the uptake behavior of NbM@EDM nanoparticles by 4T1 cells, scale bar: 20 μm. (C) Confocal microscopy images of cellular co-localization of NbM@EDM nanoparticles with lysosomes of 4T1 cells, scale bar: 40 μm.

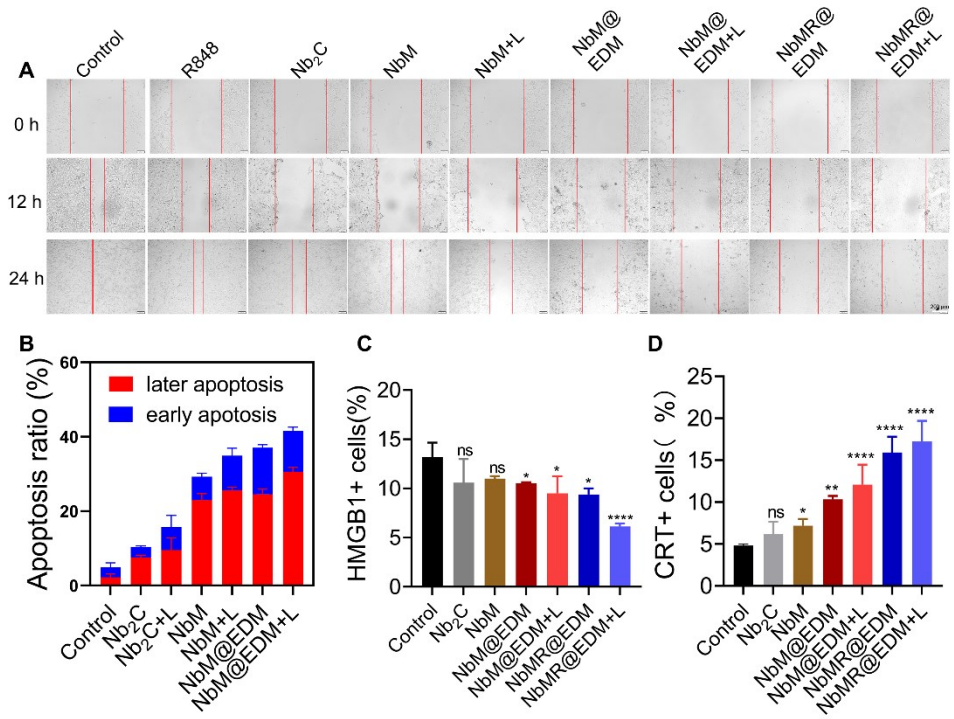

Fig. S10. (A) Scratch experiments of 4T1 cells after treatment with different conditions, scale bar: 100 μm. (B) Quantitative analysis of cell apoptosis by flow cytometry. (C) Quantitative analysis of HMGB1 expression by flow cytometry. (D) Quantitative analysis of CRT expression by flow cytometry.

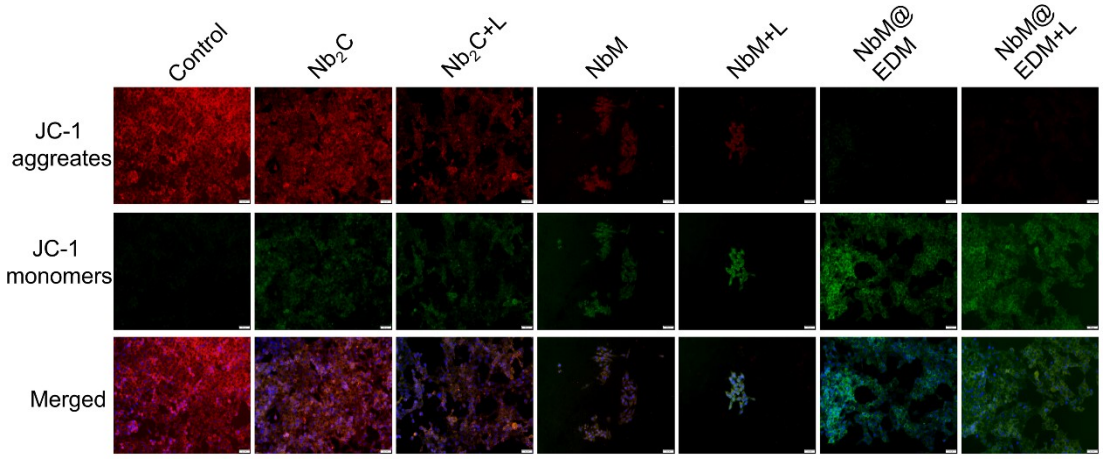

Fig. S11. Mitochondrial membrane potential of 4T1 cells after different nanoparticle treatments, scale bar: 100 μm.

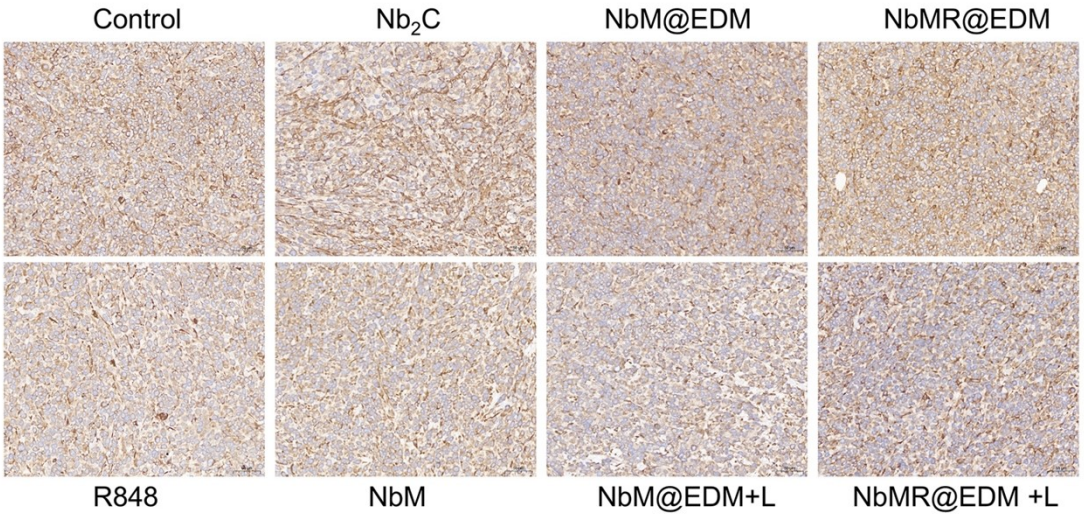

Fig. S12. CRT-stained sections of the tumor after treatment, scale bar: 100 μm.

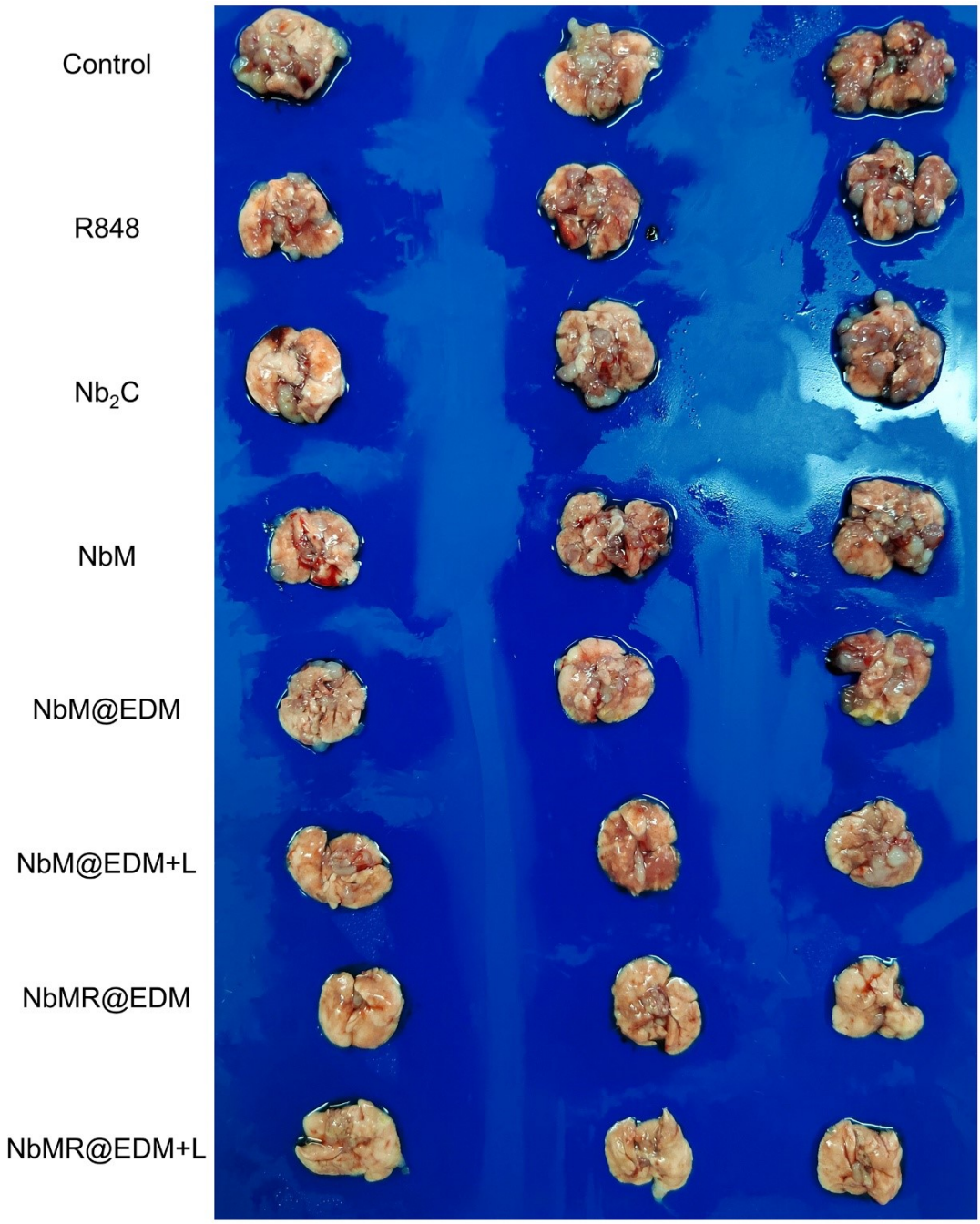

Fig. S13. Photographs of the lung after treatment.

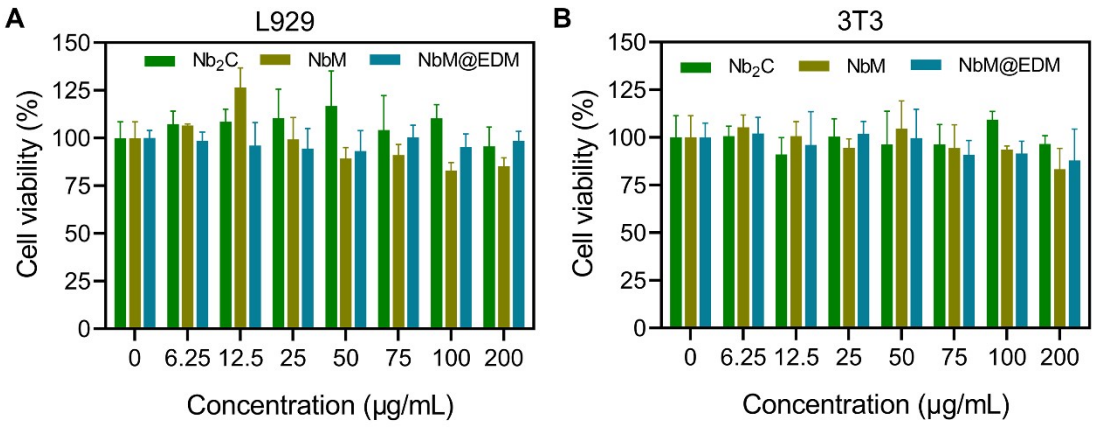

Fig. S14. Toxicity of Nb_2C, NbM and NbM@EDM on L929 cells (A) and 3T3 cells (B).

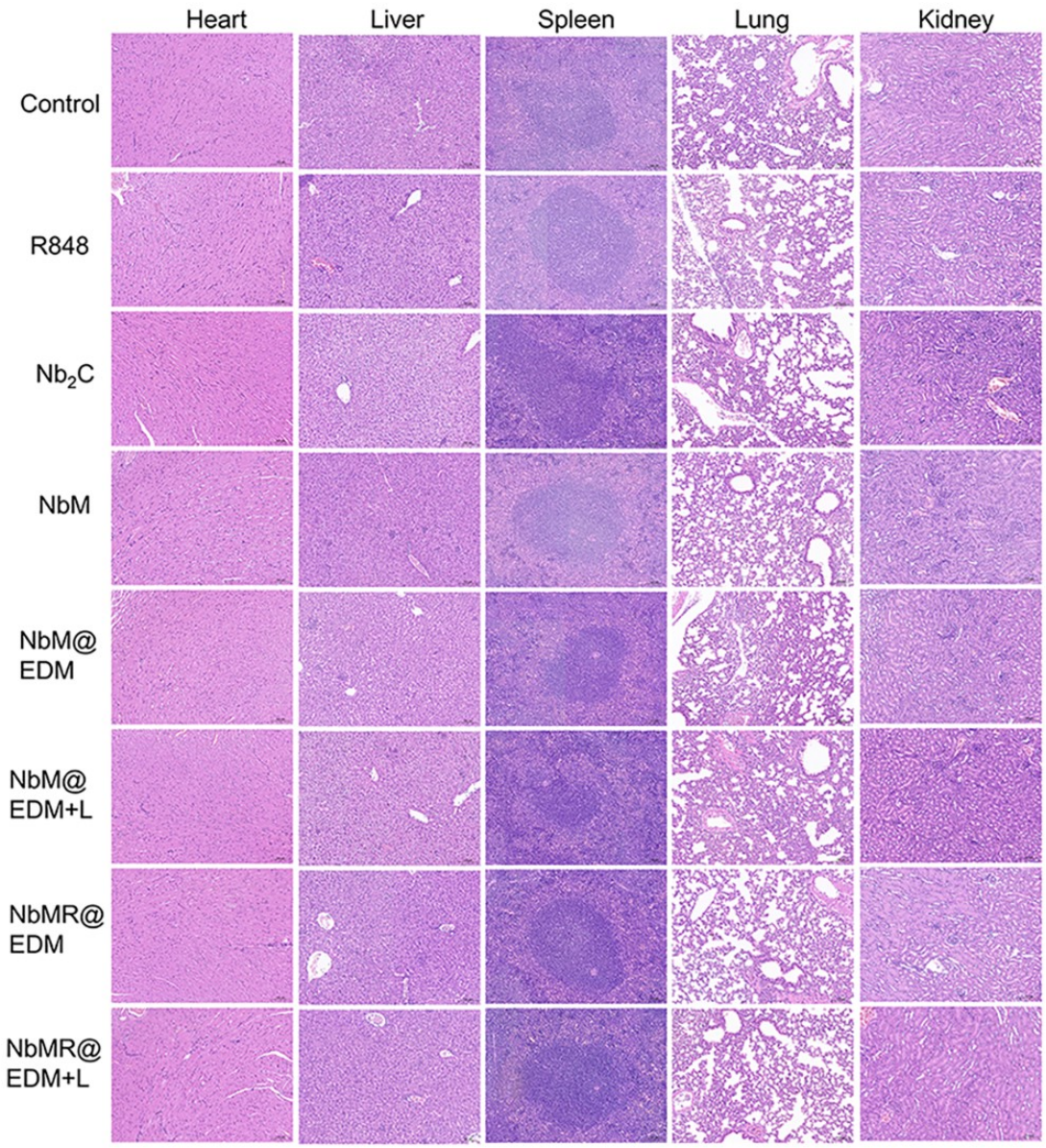

Fig. S15. H&E staining of major organs (heart, liver, spleen, lungs, kidneys) of mice after treatment, scale bar: 200 μm.

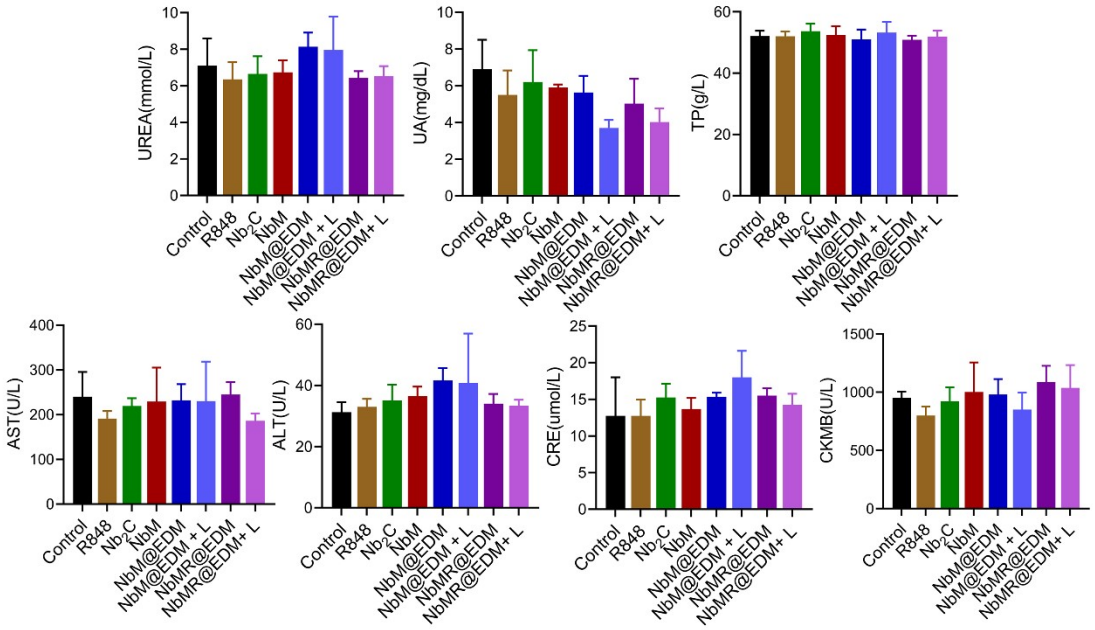

Fig. S16. Serum biochemical analysis of mice in each treatment group.

3 Table

Table S1 Data values related to the calculation of photothermal conversion efficiency η of NbM@EDM composite nanoparticles

Symbol	Values
$T_{max,H_2O} - T_{sur}$	0.4 °C
T_{max}-T_{sur}	35.1 °C
P	2.25 W
A_{808}	0.3123
slop	253.6
C_{p,H_2O}	4.2×10³ J/kg·K
hS	0.025
η	74.71 %

The formula for calculating the photothermal conversion efficiency(η) is as follows:

$$\eta = \frac{hS(T_{max} - T_{sur}) - hS(T_{max,\ H_2O} - T_{sur})}{P(1-10^{-A_{808}})} \quad (1)$$

Where T_{max} denotes the maximum temperature of the sample solution; T_{max,H_2O} denotes the maximum temperature of the solvent (water) of the sample solution; T_{sur} denotes the current environmental temperature; Q_{dis} denotes the heat loss transferred outward from the system; P denotes the laser power; A_{808} denotes the absorbance value of the sample solution at 808 nm; h denotes the heat transfer coefficient of the system; and S denotes the spot size of the laser irradiation.

The calculation formula for hS is:

$$hS = \frac{m_{\mathrm{i}} C_{\mathrm{p},i}}{\tau_{\mathrm{s}}} \tag{2}$$

Where m_i and $C_{p,i}$ denote the mass and specific heat capacity of the solvent (water); and τ_s denotes the system heat transfer time constant.

$$\tau_{\mathrm{s}} = -\frac{dt}{d\ln\theta} \tag{3}$$

Where θ is the aqueous solution driving force temperature of NbM@EDM nanoparticles and t denotes time.

The calculation formula for The aqueous solution driving force temperature θ_t at at a given moment is:

$$\theta_t = \frac{T_t - T_{sur}}{T_{\max} - T_{sur}} \tag{4}$$

So the curve between time and $ln\theta$ is plotted based on the hydrodynamic temperature θ_t at different time, and the negative of the slope of this regression line, i.e., the system heat transfer time constant τ_s, is calculated.